

# Inhibition of Kinesin-5, a Microtubule-Based Motor Protein, As a Strategy for Enhancing Regeneration of Adult Axons

Shen Lin<sup>1</sup>, Mei Liu<sup>1,2</sup>, Young-Jin Son<sup>1</sup>,  
Barry Timothy Himes<sup>1,3</sup>, Diane M. Snow<sup>4</sup>,  
Wenqian Yu<sup>1</sup> and Peter W. Baas<sup>1,\*</sup>

<sup>1</sup>Department of Neurobiology and Anatomy, Drexel University College of Medicine, 2900 Queen Lane, Philadelphia, PA, USA

<sup>2</sup>Jiangsu Key Laboratory of Neuroregeneration, Nantong University, Nantong, Jiangsu, China

<sup>3</sup>Department of Veterans Affairs Hospital, Philadelphia, PA, USA

<sup>4</sup>Spinal Cord and Brain Injury Research Center and Department of Anatomy and Neurobiology, University of Kentucky, Lexington, KY, USA

\*Corresponding author: Peter W. Baas,  
pbaas@drexelmed.edu

**Developing neurons express a motor protein called kinesin-5 (also called kif11 or Eg5) which acts as a 'brake' on the advance of the microtubule array during axonal growth. Pharmacological inhibition of kinesin-5 causes the developing axon to grow at a faster rate, retract less and grow past cues that would otherwise cause it to turn. Here we demonstrate that kinesin-5 is also expressed in adult neurons, albeit at lower levels than during development. We hypothesized that inhibiting kinesin-5 might enable adult axons to regenerate better and to overcome repulsive molecules associated with injury. Using adult mouse dorsal root ganglion neurons, we found that anti-kinesin-5 drugs cause axons to grow faster and to cross with higher frequency onto inhibitory chondroitin sulfate proteoglycans. These effects may be due in part to changes in the efficiency of microtubule transport along the axonal shaft as well as enhanced microtubule entry into the distal tip of the axon. Effects observed with the drugs are further enhanced in some cases when they are used in combination with other treatments known to enhance axonal regeneration. Collectively, these results indicate that anti-kinesin-5 drugs may be a useful addition to the arsenal of tools used to treat nerve injury.**

**Key words:** axon, cytoskeleton, Eg5, kinesin-5, microtubule, monastrol, nerve, neuron, regeneration

Received 26 August 2010, revised and accepted for publication 15 December 2010, uncorrected manuscript published online 17 December 2010, published online 17 January 2011

When injured, the axons of adult neurons regenerate moderately well outside of the central nervous system (CNS). However, within the CNS environment, the regeneration of injured axons is minimal at best, and this is true whether the axon arises from a neuron of the CNS

or a neuron of the peripheral nervous system (PNS) (1,2). Extrinsic factors that contribute to failure of axonal regeneration in the CNS include inhibitory chondroitin sulfate proteoglycans (CSPGs), which are a major constituent of the glial scar (3), myelin components such as Nogo, MAG and Omgp (4) and decreased levels of growth factors (5). Growth of injured adult axons is also suboptimal compared to developing axons because the machinery for growth is simply not as robust (6).

Axons are characterized by dense arrays of cytoskeletal elements that provide architectural support and also act as railways for the transport of various classes of cargo. The cytoskeletal elements themselves also undergo transport within the axon. It was posited years ago that the rates of axonal growth are dependent upon the vitality of the transport of the cytoskeletal elements (7). Unfortunately, not enough was known about these mechanisms to translate into effective clinical strategies for treating patients with nerve injuries. Today, however, more is known, especially about the transport of microtubules in developing axons. It has been shown that only very short microtubules undergo rapid sustained transport (8). Interestingly, the same motors that influence the transport of the short microtubules impose forces on the longer ones that determine whether the axon grows or retracts and also enable the axon to turn properly in response to environmental cues (9).

Particularly intriguing are recent observations on kinesin-5 (also known as kif11, Eg5 or KSP), a homotetrameric motor protein that generates forces between neighboring microtubules (10). In developing neurons, inhibition of kinesin-5 increases the number of short microtubules in transit, causes axons to grow faster and retract less, and also permits axons to grow past signals that would normally cause them to turn (11,12). In theory, these effects (which we have likened to releasing a 'brake' on axonal growth) could be ideal for assisting the axons of adult neurons to regenerate with more vitality after injury. Here, to investigate this possibility, we tested for the presence of kinesin-5 in neurons of the adult CNS and PNS, and also ascertained whether inhibiting kinesin-5 with available drugs enables the axons of cultured adult neurons to regenerate better.

## Results

### *Expression of kinesin-5 in the adult nervous system*

Kinesin-5 is best known as a mitotic motor. On the basis of the potent anti-proliferative effects of inhibiting kinesin-5 and the assumption that kinesin-5 is absent

from the nervous system, drug companies have sought to expand the repertoire of anti-kinesin-5 drugs for use in cancer treatment (13,14). In our original study showing that kinesin-5 is expressed in terminally postmitotic neurons, we reported that kinesin-5 mRNA levels are barely detectable in the adult nervous system of rodents (15). We have now confirmed this result, and extended it to show that mRNA levels decrease during development. In addition, we have, for the first time, investigated kinesin-5 protein levels in the development of adult mouse nervous system. We found that there is a decrease in kinesin-5 protein during development. However, kinesin-5 protein levels decrease at a slower rate than mRNA levels with some kinesin-5 protein still remaining in the adult PNS and CNS.

For the present studies, the levels of kinesin-5 mRNA and protein were analyzed in cerebral cortex, spinal cord and DRGs (dorsal root ganglia) at four different ages of mice. These studies were performed using semi-quantitative real-time polymerase chain reaction (RT-PCR) and western blotting, respectively. RT-PCR showed that kinesin-5 mRNA was much higher in the cortex at P3 compared with the adult while the control glyceraldehyde-3-phosphate dehydrogenase (GAPDH) mRNA levels remained the same. The greatest reduction in expression occurred in the first few postnatal weeks, where mRNA expression in the cortex dropped from P1 to adult by over 90% (Figure 1A). This correlates with kinesin-5 protein levels, which also dramatically decreased in the cortex during the first two postnatal weeks (Figure 1B), decreasing from P1 to adult by over 70% (P1  $0.877 \pm 0.184$ ; adult  $0.240 \pm 0.059$ , normalized band intensity  $\pm$  SEM, paired student's *t*-test). Levels of kinesin-5 also decreased by around 60% in the spinal cord (P1  $0.548 \pm 0.041$ ; adult  $0.212 \pm 0.064$ ) and in the DRG by around 85% (E18  $0.384 \pm 0.098$ ; adult  $0.060 \pm 0.028$ ) but consistently remained lower than in the cortex. The greatest decrease in the levels of kinesin-5 occurred during development in the DRG, indicating that kinesin-5 is lost more quickly during development in the PNS compared to the CNS. Confirming the identity of the relevant band on our western blots as kinesin-5, the same antibody used on the mouse tissues detected a band of identical mobility in rat fibroblast cell line (RFL-6), and this band was diminished after treatment of the cells with kinesin-5 siRNA but not control siRNA (Figure 1B). No significant changes were seen in the GAPDH internal control (Figure 1B).

Gene expression in neurons often changes following injury to re-establish the plasticity that occurs during development (16). In a general survey of kinesin mRNA levels after dorsal root crush, there were no reported changes in the mRNA for kinesin-5 (17). Here, we wished to investigate this at the protein level. The growth potential of the DRGs was enhanced by crushing their peripheral axons 10 days before crushing dorsal root axons. The kinesin-5 levels were analyzed by western blotting 2 days after the second crush (Figure 1C). Levels of kinesin-5 showed an apparent decrease in the cortex but the apparent decrease

was not statistically significant (Figure 1D). Changes in kinesin-5 levels in the sciatic nerve (Figure 1E), spinal cord (Figure 1F) and DRG (Figure 1G) were also not statistically significant ( $n = 3$ , paired student's *t*-test).

The limitation of RT-PCR and western blots is that tissue homogenates contain various other cell types in addition to neurons. Some of these cells are mitotic, and hence, would certainly be expected to express kinesin-5. In order to test whether the results observed with the western blots accurately depict kinesin-5 expression within neurons, we conducted immunohistochemical analyses on adult tissues. This approach confirmed that kinesin-5 is expressed in the cell bodies of the DRGs, in the neuronal cell bodies of the spinal cord gray matter and also in the axons projecting into the sciatic nerve (Figure 2). This shows that kinesin-5 is expressed in the adult CNS and PNS neurons. In the negative control where only the secondary antibody was incubated with the tissue, equal amounts of background staining were observed in all of the tissues examined (Figure 2). Additional confidence in the specificity of the primary antibody was provided by cell culture work in which staining with the antibody was strongly reduced in cells depleted of kinesin-5 by siRNA (data not shown; see also Ref. 12). Double-immunostaining analysis of kinesin-5 in injured neuronal tissues showed analogous staining patterns to normal tissues in the DRG, spinal cord and sciatic nerves (Figure 3A–D). There was a decrease in the staining intensity of injured DRGs, spinal cord and the proximal sciatic nerve compared with control tissue from non-injured animals, but this decrease was also statistically insignificant (Figure 3E–G). While we did not test for potential changes in kinesin-5 levels at longer times after the lesion, the fact that no detectable change occurred after 2 days suggests that there should be at least some kinesin-5 present at longer times as well.

#### ***Inhibition of kinesin-5 increases axonal length***

For functional analyses, we chose not to use RNAi methods on adult neurons because the mRNA for kinesin-5 is already very low, and because the drug approach is the one most translatable to the clinic. While mRNA levels in adult neurons are less than 10% of juvenile levels, protein levels in adult DRG and spinal cord tissue are still 15 and 40%, respectively, compared with juvenile levels. We used three different kinesin-5 inhibitors, namely monastrol (18), *S*-trityl-L-cysteine (STLC) (19) and HR22C16 (20). We used cultured DRG neurons because they have been used extensively for studies on axonal regeneration, and because they are a good model for conditional dorsal root injury *in vitro* (21). Moreover, to the best of our knowledge, they are the only type of adult neuron that can be readily cultured with straightforward techniques.

DRG neurons obtained from young adult mice were grown on laminin for 18 h, during which time they grew axons. The cultures were then fixed and processed for immunocytochemistry for morphological analyses. All cells showed robust axonal outgrowth during the first

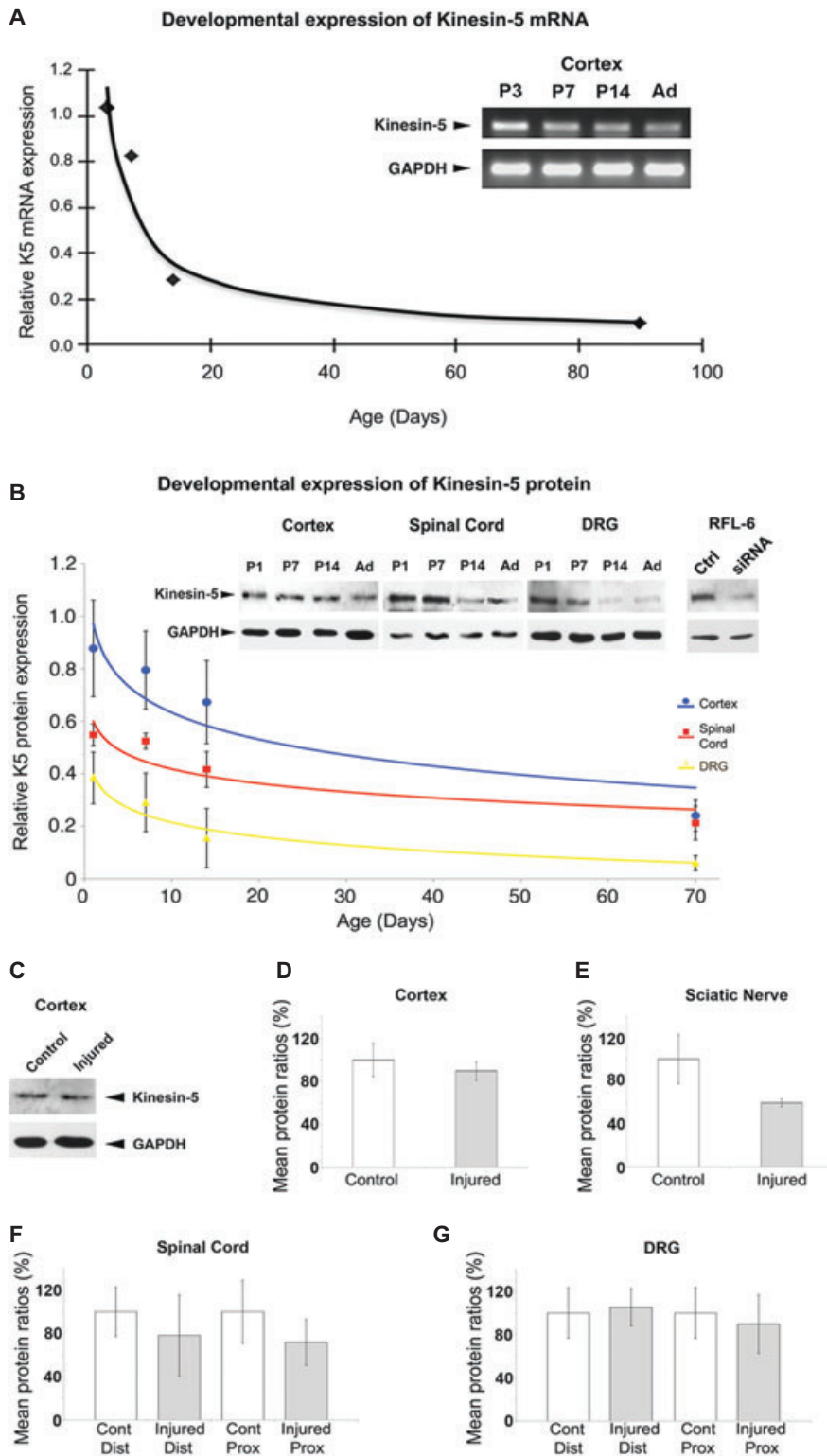


**Figure 1: Kinesin-5 mRNA and protein levels decrease during the development in CNS and PNS tissues.**

A) RT-PCR showing kinesin-5 mRNA levels in rat cortex at P3, P7, P14 and 3 months old (Ad, see inset). Real-time RT-PCR analysis shows a downregulation of kinesin-5 mRNA in the cortex as the animal ages. B) Tissues (cortex, spinal cord and DRG) were collected from mice at P1, P7, P14 and 10 weeks old (Ad). RFL-6 cells electroporated with control and kinesin-5 siRNA were collected after 2 days in culture. Protein extracts from each time-point were used for western blotting. Kinesin-5 decreases as the mouse ages, but GAPDH remains constant in the cortex, spinal cord and DRGs. Kinesin-5 levels are notably higher in RFL-6 cells treated with control siRNA compared to cells treated with kinesin-5 siRNA (see inset). ODs were measured for bands representing kinesin-5 in neuronal tissues, and protein concentrations were read from standard curves. In the cortex, spinal cord and DRG, kinesin-5 OD ratio decreased mostly in the first few postnatal weeks. C) Representative western blot of mouse cortex (5 g) collected from non-injured adult mice (control) and injured mice were probed with anti-kinesin-5 antibody and GAPDH as the loading control. D–G) Values are plotted as a percentage representing the normalized mean of three independent experiments, relative to the protein levels of corresponding control tissue from non-injured mouse (defined as 100%), with bars representing SEM. Kinesin-5 expression appears to be slightly reduced after injury in the cortex (D), sciatic nerve (E), the spinal cord (F) and proximal DRGs (G) compared with control tissues from non-injured mice. However, there is no statistically significant loss of kinesin-5 protein after injury in any of the tissues examined (paired student's *t*-test).

18 h of plating, often extending more than a dozen axons from each cell body (Figure 4A). All of the processes are axonal in character as confirmed by the uniform polarized orientation of their microtubules and their staining

with the tau-1 antibody (data not shown). In order to analyze overall axonal growth, we measured the four longest axons from each neuron and calculated the total length for neurons in each condition. Cultures treated

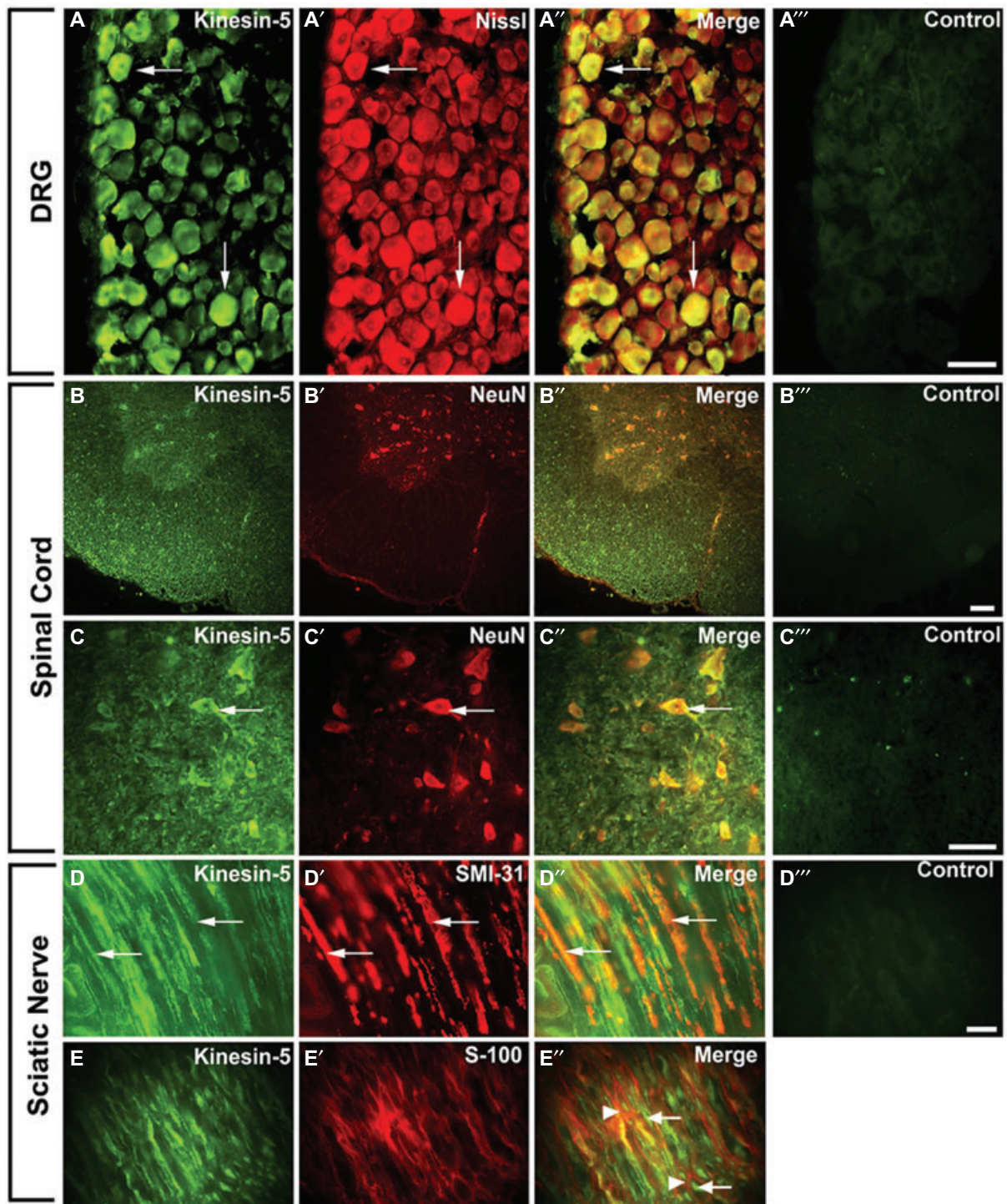


**Figure 2: Kinesin-5 in adult DRG, spinal cord and sciatic nerves.** A) Immunostaining for kinesin-5 in L5 DRG neurons shows kinesin-5 is present in the cell bodies and colocalizes with the fluorescent Nissl stain (A', arrows). Bar, 50  $\mu$ m. B) Immunostaining for kinesin-5 in L5 transverse spinal cord cross-section shows kinesin-5 is present together with NeuN (B'), a neuronal marker in the white matter and gray matter neurons on the ventral side. Bar, 50  $\mu$ m. C) Higher magnification of a region in the gray matter shows kinesin-5 colocalizes with neurons labeled by NeuN (C', arrows). D) Immunostaining for kinesin-5 in longitudinal sections of the sciatic nerve show that kinesin-5 is present in the axons and colocalizes with SMI-31R (D'), which labels axonal neurofilaments (arrows; upper panels). E) Kinesin-5 is present in the axon (arrows) but not Schwann cells (arrowheads), labeled by S-100 (E'). Kinesin-5 labeling is specific in adult DRG, spinal cord and sciatic nerves. In controls where the primary antibody is omitted, there is very little fluorescence in the DRGs (A'''), spinal cord lower magnification (B'''), spinal cord higher magnification (C''') and sciatic nerves (D'''). A–C bars, 50  $\mu$ m; D bar, 10  $\mu$ m.

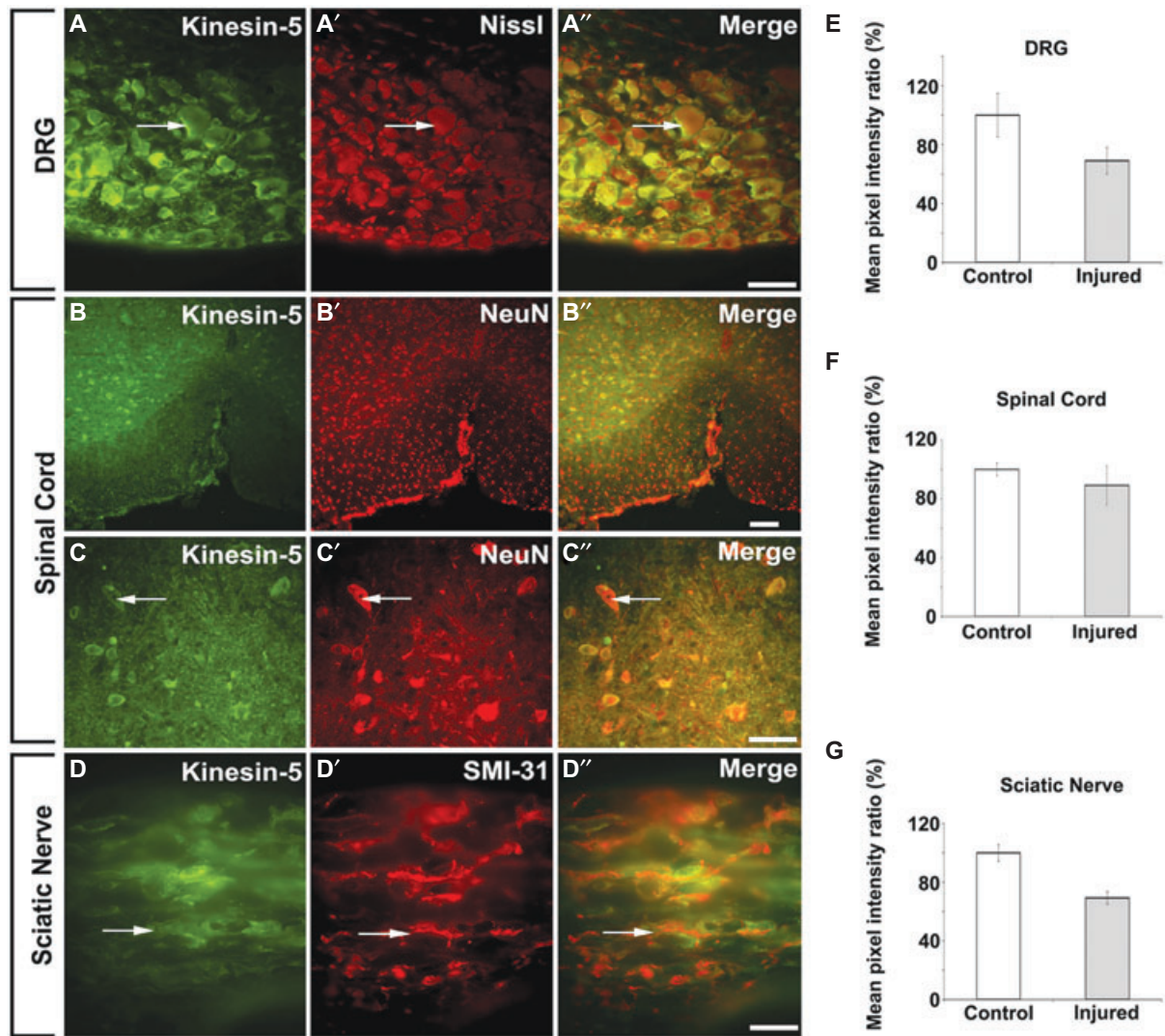


**Figure 3: Kinesin-5 in neurons of the DRG, spinal cord and sciatic nerve after dorsal root injury.** A–D) Immunostaining for kinesin-5 in injured animals shows kinesin-5 is still present in the L5 DRG cell bodies (A, arrows) and L5 level spinal cord neurons (B, arrows), colocalizing with fluorescent Nissl stain (A') and with the neuronal marker NeuN (B'), respectively. Bar, 50  $\mu$ m. C) Higher magnification of a region in the spinal cord also shows colocalization of kinesin-5 with NeuN (C'). Bar, 50  $\mu$ m. D) Immunostaining for kinesin-5 in the crushed proximal sciatic nerve shows that it is present in the axons and colocalizes with the axonal neurofilament marker SMI31R (D'). Bar, 10  $\mu$ m. E–G) Quantification of kinesin-5 mean fluorescence intensity (green) in non-injured and injured animals. Values are plotted as a percentage representing the normalized mean of at least five independent measurements from three experiments, relative to the intensity levels of corresponding control tissue from non-injured mouse (defined as 100%), with bars representing SEM. Kinesin-5 appears to decrease slightly in DRGs (E), the spinal cord (F) and sciatic nerve (G) compared with controls, but these differences are not statistically significant.

with anti-kinesin-5 drugs all exhibited longer axons compared with controls (Figure 4B). In monastrol-treated cultures, the four longest axons grew to  $545.40 \pm 26.33$   $\mu$ m;  $p < 0.01$  ( $n = 30$ ), in STLC-treated cultures, to  $561.94 \pm 31.76$   $\mu$ m;  $p < 0.01$  ( $n = 26$ ) and in HR22C16-treated cultures, to  $602.74 \pm 38.26$   $\mu$ m;  $p < 0.001$  ( $n = 35$ ), significantly longer than the neurons treated with dimethyl sulfoxide (DMSO) control,  $431.11 \pm 31.92$   $\mu$ m ( $n = 24$ ; mean  $\pm$  SEM; paired student's  $t$ -test, assuming unequal variances). To obtain a sample of the proportion

of neurons with long and short axons, we measured the longest axon from each neuron. In monastrol-treated cultures, up to 65% of neurons grew axons between 100  $\mu$ m and 200  $\mu$ m and in HR22C16-treated cultures this proportion was similar at 59% (Figure 4C). However, in STLC-treated cultures, almost 50% of neurons grew axons that extended beyond 200  $\mu$ m. In cultures treated with no drugs, only 36% of neurons grew axons between 100  $\mu$ m and 200  $\mu$ m. These results show that

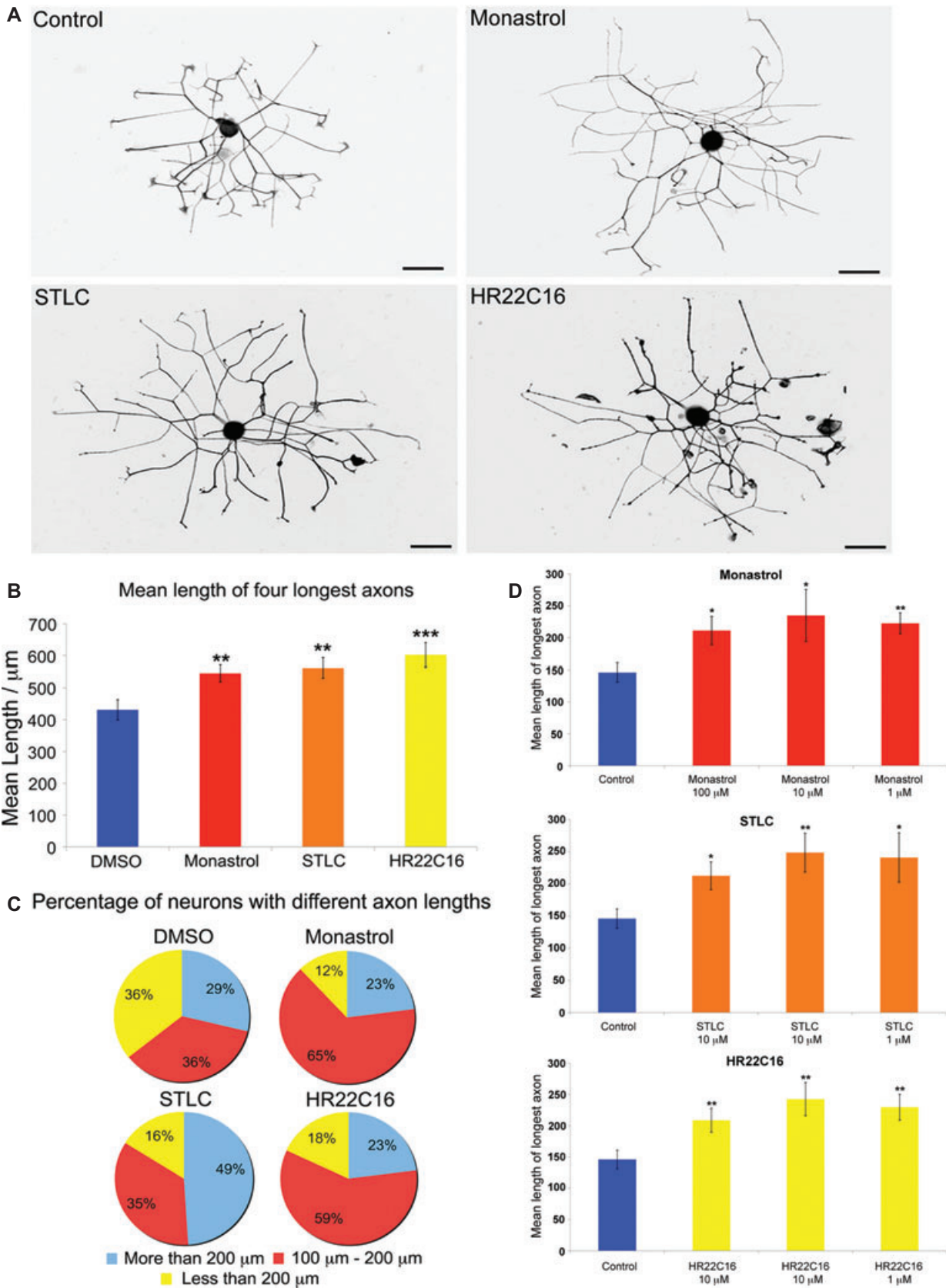


Figure 4: Legend on next page.

anti-kinesin-5 drugs vary a bit in their impact, but clearly have growth-promoting effects on adult axons.

Previous studies have shown that low concentrations of kinesin-5 inhibitors can significantly inhibit activity of kinesin-5 and have  $IC_{50}$  values much lower than the ones used in this investigation (18–20). We used higher concentrations in order to show that adult neurons can tolerate such doses, given that *in vivo* regimes may require drugs to be used at higher concentrations than when applied directly to neurons in culture. Toxicity at higher doses could present a problem with *in vivo* regimes. To ascertain whether the results with the higher concentrations are any more robust or less robust than with lower concentrations, we performed additional experiments with monastrol, STLC and HR22C16 at three different concentrations for 10 h in DRG cultures. In all cases, axons were significantly longer in drug-treated cultures compared with control cultures (Figure 4D). However, there was no significant difference in axonal length among the various drug concentrations used. There was also no visible difference in neuronal survival or other morphological changes at the various drug concentrations used. These results indicate that lower doses may be sufficient to elicit the same effects as higher doses but also that higher doses do not impose detectable toxicity problems.

#### **Inhibition of kinesin-5 enables axons to overcome inhibitory CSPG borders**

CSPGs are the major component of the glial scar following injury that inhibits regenerating axons from crossing over to establish new connections (22,23). To investigate the effects of different kinesin-5 inhibitors on DRG neurons growing toward inhibitory substrates, an *in vitro* model of the glial scar was used in which axons were challenged to cross a border from laminin onto various concentrations of CSPG. Adult DRG neurons were dissociated, plated onto the laminin side of the culture, incubated with or without anti-kinesin-5 drugs for 2 days in culture and then fixed. At 25  $\mu$ g/mL of CSPG, the lowest concentration used, axons generally did not cross the inhibitory border (Figure 5A) and remained on the laminin side where they either avoided or turned away from the border upon contact. In the presence of monastrol ( $n = 6$ ), there was more than 120% increase in the proportion of axons ( $p < 0.01$ ) crossing the CSPG border. These axons crossed the border and continued growing (Figure 5B). At 50  $\mu$ g/mL of CSPG, most axons also failed to cross

the CSPG border (Figure 5C), but addition of monastrol also increased crossing by twofold ( $p < 0.05$ ; Figure 5D). However, in the presence of monastrol, the proportion of axons that managed to cross the 50  $\mu$ g/mL CSPG border was slightly less than that which crossed the 25  $\mu$ g/mL border (Figure 5E). This proportion decreased as the concentration of CSPG increased beyond 100  $\mu$ g/mL. There was no significant difference in axonal crossing between neurons treated with DMSO or with monastrol when axons encountered 100 or 200  $\mu$ g/mL CSPG (Figure 5E; mean  $\pm$  SEM; unpaired student's *t*-test).

Application of STLC ( $n = 3$ ) caused a 130% increase in the proportion of axons growing past 25  $\mu$ g/mL CSPG border ( $p < 0.001$  and 0.01, respectively), slightly greater than the response with monastrol (Figure 5E; mean  $\pm$  SEM; unpaired student's *t*-test). Interestingly, STLC significantly raised the proportion of axonal crossings at 100  $\mu$ g/mL ( $p < 0.001$ ) and 200  $\mu$ g/mL ( $p < 0.001$ ) CSPG, which monastrol failed to do. HR22C16 ( $n = 3$ ), although less effective at promoting axonal growth at 25  $\mu$ g/mL of CSPG, significantly raised the crossover ratio at 50, 100 and 200  $\mu$ g/mL ( $p < 0.01$ , 50  $\mu$ g/mL;  $p < 0.001$ , 100  $\mu$ g/mL and  $p < 0.001$ , 200  $\mu$ g/mL). This suggests that, while monastrol can increase the ability of regenerating axons to cross onto lower concentrations of CSPG, STLC and HR22C16 can do this better at higher concentrations. Thus, as with the results on axonal growth, there was some variability with the three drugs, but the impact was positive with each of the drugs.

#### **ChABC treatment further increases the effects of monastrol**

The enzyme ChABC (chondroitinase ABC), which degrades CSPG glycosaminoglycan (GAG) chains, has been used with varying degrees of success *in vivo* to modify injured environments (24), with the goal of encouraging axons to cross the injury site so that they can grow back to their original targets (25). However, in a clinical setting, the effects of ChABC may be limited by certain factors such as quick loss of thermostability at body temperature (26) and the lack of diffusion after intrathecal injection (27). To investigate whether a combination of ChABC and an anti-kinesin-5 drug treatment could further improve axonal regeneration in our *in vitro* model, DRG neurons were cultured with or without monastrol ( $n = 3$ ) against CSPG stripes that has been predigested with ChABC. A concentration of 0.1 U ChABC was used and incubated with

**Figure 4: Inhibition of kinesin-5 increases the rate of axonal growth and axonal density.** A) DRG neurons treated with DMSO, monastrol, STLC or HR22C16 were grown in culture for 18 h. Bar, 40  $\mu$ m. B) Monastrol (red bar), STLC (orange bar) and HR22C16 (yellow bar) significantly increased the mean of the four longest axons. C) Percentage of neurons treated with DMSO, monastrol, STLC or HR22C15 in which the length of the longest axon is less than 100  $\mu$ m (yellow), 100–200  $\mu$ m (red) or more than 200  $\mu$ m (blue). D) Increase in axonal growth is similar at different drug concentrations. DRG neurons treated with DMSO, monastrol, STLC or HR22C16 were grown for 10 h. Monastrol significantly increased the length of the longest axon in neurons compared to control cultures, but the increase was equally great at 100, 10 or 1  $\mu$ M. Similarly, STLC and HR22C16 significantly increased the length of the longest axon compared to control, but the increase was relatively the same at 10, 5 or 1  $\mu$ M. \* $p < 0.05$ , \*\* $p < 0.01$ , \*\*\* $p < 0.001$ . These results indicate that all of these drug concentrations are higher than needed to optimally suppress kinesin-5, but still display no detrimental effects on the health of the neuron.

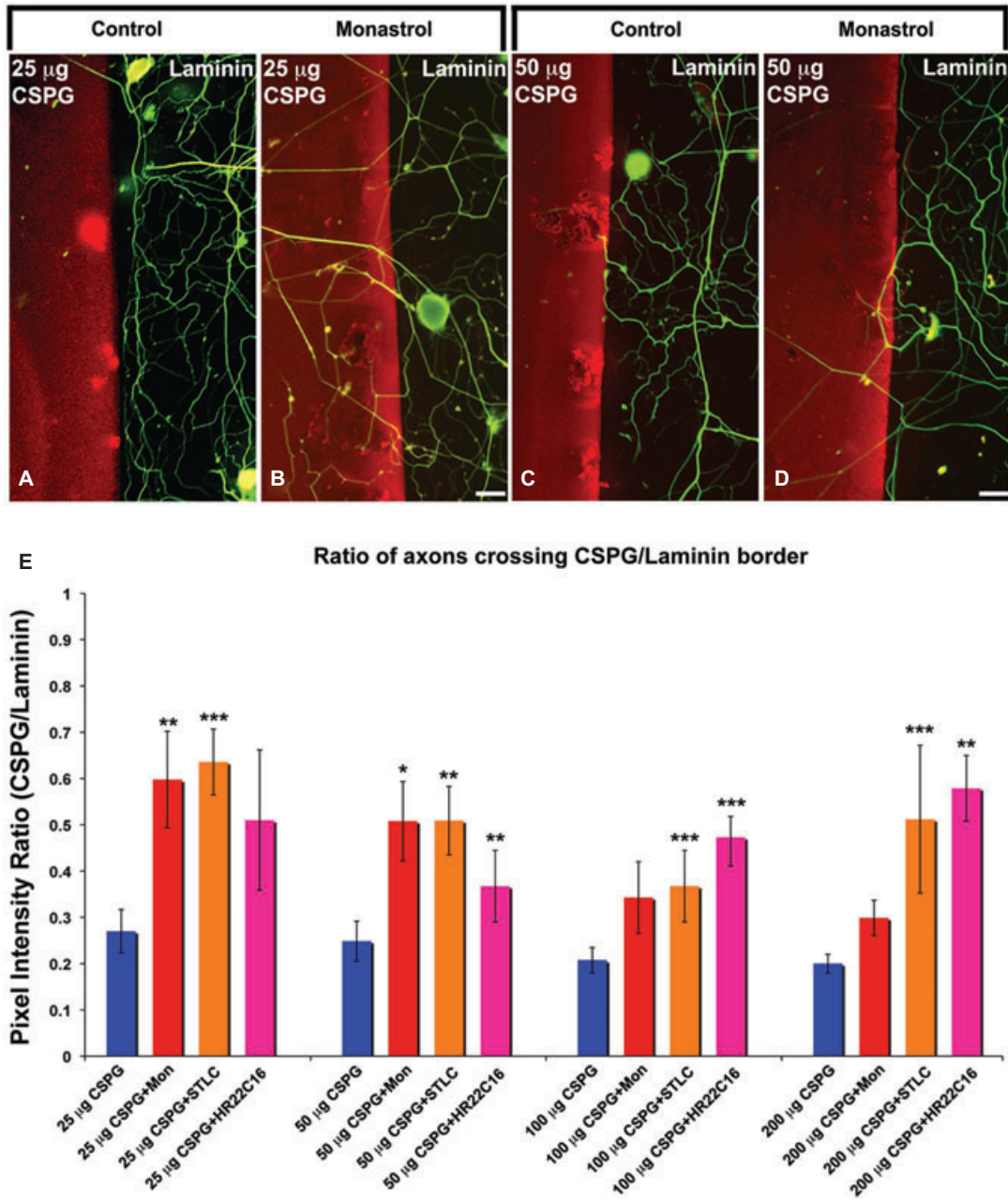


**Figure 5: Effects of anti-kinesin-5 drugs on axonal crossing over inhibitory borders.** A–D) Representative images of DRG axons labeled with  $\beta$ -III tubulin (green) plated on laminin and growing toward the CSPG border (red). Bar, 20  $\mu$ m. A and C) Most control axons turn at the border or grow a very small distance into the CSPG. B and D) Monastrol-treated axons grow robustly into the substrate. E) Quantification of axons crossing the inhibitory CSPG border, measured by the mean pixel intensity of axons labeled by  $\beta$ -III tubulin on the CSPG side/laminin side. Monastrol (red bars) causes significantly more crossover of axons compared with controls (blue bars) at lower concentrations of CSPG. STLC (orange bars) significantly increased the crossing over of axons compared to controls at all concentrations of CSPG, while HR22C16 (purple bars) increased crossover in all except the lowest CSPG concentration, \* $p < 0.05$ , \*\* $p < 0.01$ , \*\*\* $p < 0.001$ .

CSPG stripes for just 3 h in order to allow some CSPG to remain after digestion and still be detected by the CS-56 antibody (Figure 6A,B). We took this approach because a full digestion would have eliminated the border and encouraged nearly all axons to grow over the remaining

CSPG sugar stub, confounding any observable effects of monastrol in boosting axonal growth. The results showed that treatment with ChABC significantly improved axonal growth over the inhibitory border across the range of concentrations of CSPG compared to the control cultures ( $p <$

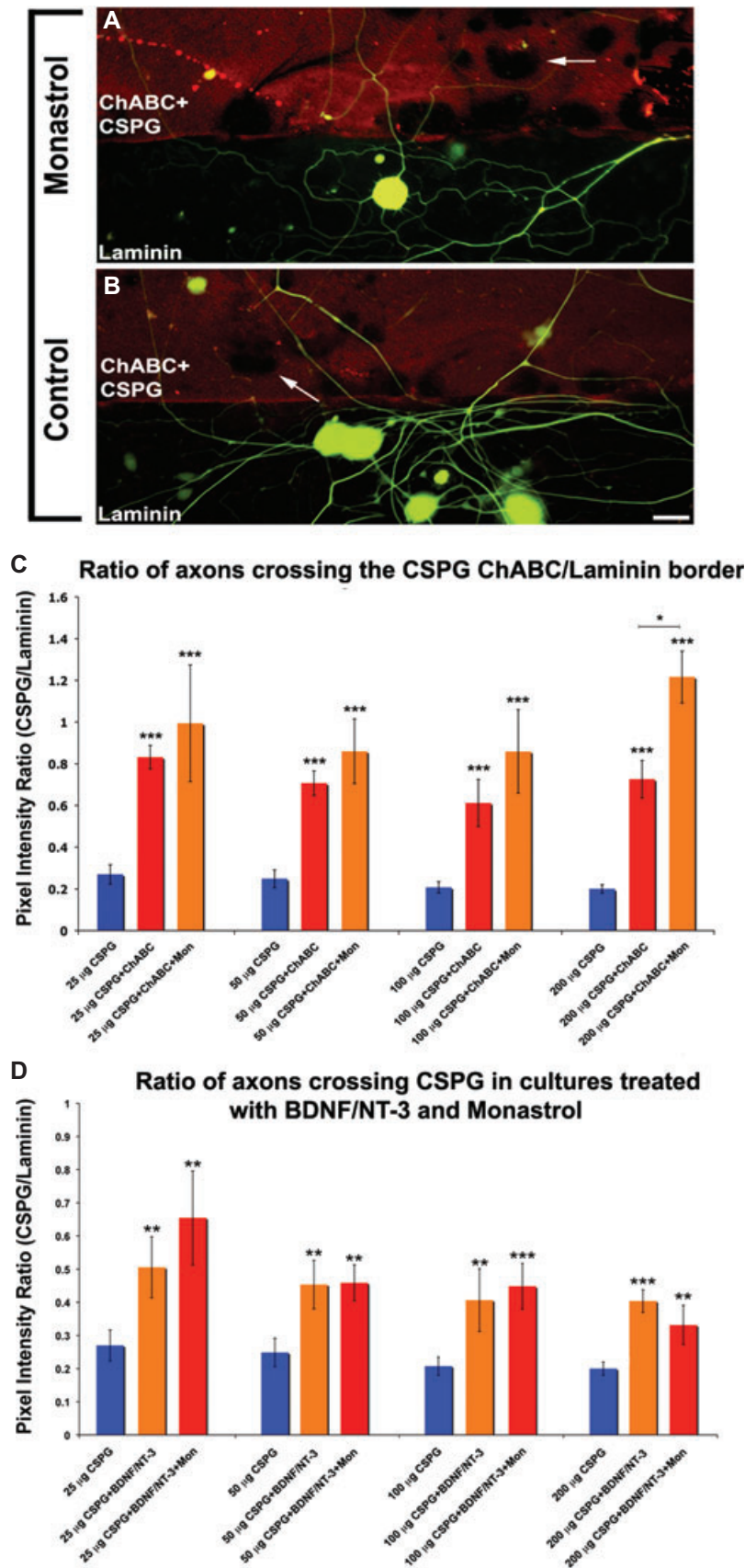


**Figure 6: Effects of combining monastrol, ChABC and neurotrophic factors on axonal crossover onto substratum-bound CSPG.** A and B) Representative images of DRG axons (green) plated on laminin and growing toward the ChABC-treated CSPG border (red). A) Some thin axons turned at the border and some grew onto the CSPG. B) Many axons grew robustly onto the CSPG. The partial ChABC digestion changes the fluorescence pattern of parts of the CSPG stripe (arrows). Bar, 20 µm. C) Quantification of axons crossing over the partially digested CSPG border measured by the mean pixel intensity of axons labeled by β-III tubulin on the CSPG side/laminin side. The greatest number of axons crosses with combinatorial treatment. ChABC + monastrol (orange bars) causes a greater increase in axonal crossing than ChABC alone at 200 µg CSPG (red bars). D) Addition of BDNF/NT-3 alone to the culture caused an increase in axonal crossing at all concentrations of CSPG (red bars) compared with control (blue bars). BDNF/NT-3 coupled with monastrol (orange bars) also significantly increases axonal crossing compared with control, but the increase was not significantly greater compared to BDNF/NT-3 treatment or to monastrol alone, \**p* < 0.05, \*\**p* < 0.01, \*\*\**p* < 0.001.

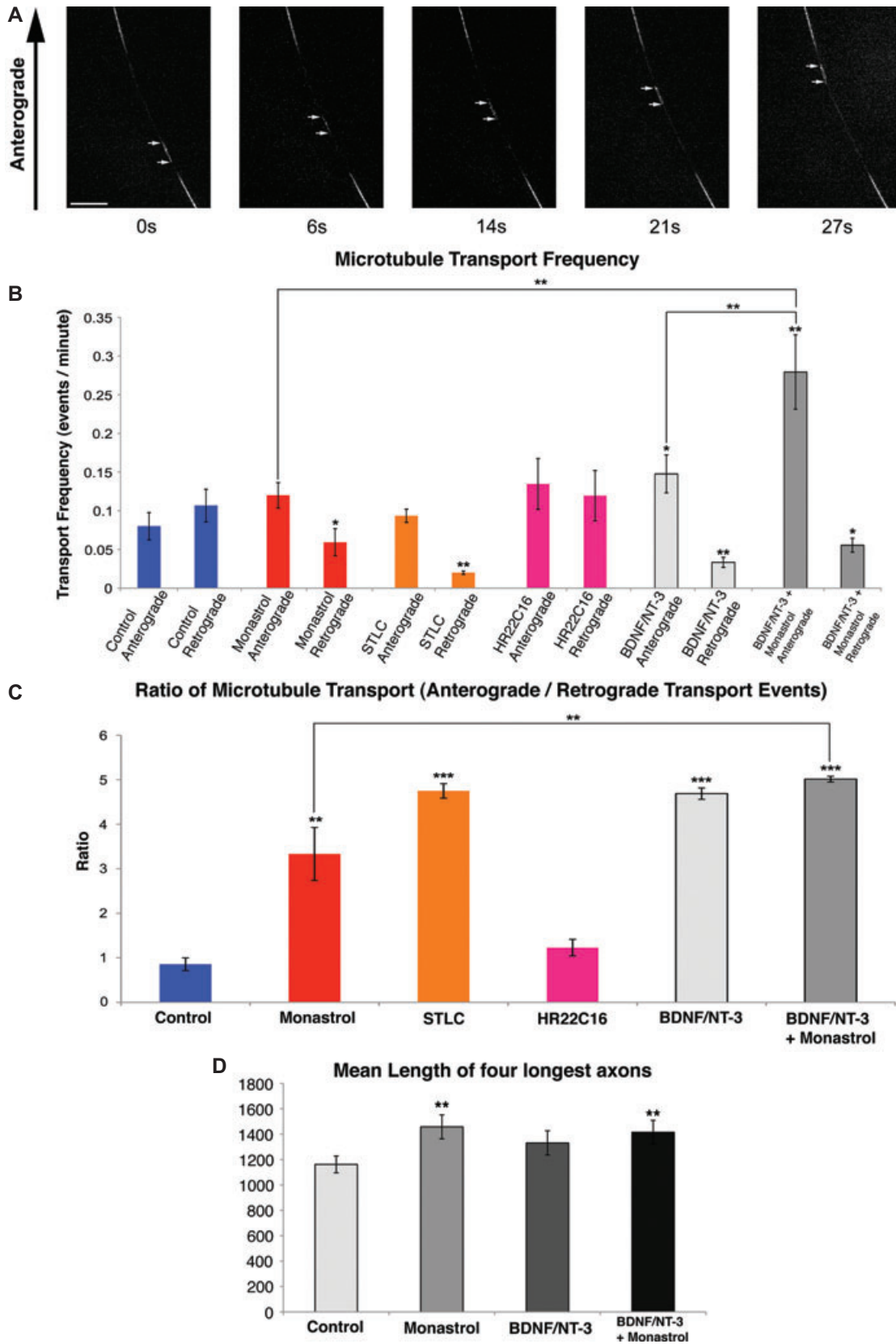


Figure 7: Legend on next page.

0.001, all CSPG concentrations) (Figure 6C). This increase was further enhanced, by 67%, when axons encountered 200  $\mu$ g/mL CSPG ( $p < 0.05$ ) compared with no monastrol (mean  $\pm$  SEM; unpaired student's  $t$ -test). This suggests that a combinatorial regime of inhibiting kinesin-5 while also diminishing the contribution of CSPG GAG chains results in an additive effect that promotes further axonal outgrowth over CSPGs. This is especially true at higher concentrations of CSPG, which are typical of glial scars.

#### **Combinatorial treatment of neurotrophic factors with monastrol**

Previous studies have shown that a variety of neurotrophic factors improve axonal growth on inhibitory substrates (28). To test if combining neurotrophic factors and inhibiting kinesin-5 could further promote axonal growth on the inhibitory border assay, DRG cultures were incubated with brain-derived neurotrophic factor (BDNF) and neurotrophin-3 (NT-3) with or without monastrol ( $n = 3$ ). The media for these studies already contained NGF (nerve growth factor) so this growth factor was not added as an extra supplement. The axonal crossing significantly increased by 88% after addition of BDNF and NT-3 in cultures with 25  $\mu$ g/mL CSPG stripes ( $p < 0.01$ ) compared to controls (Figure 6D). Addition of monastrol together with BDNF and NT-3 to the media raised the proportion of axonal crossing relative to controls by 140%, thus having a greater effect compared to incubation with growth factors alone. While at higher concentrations of CSPG, the combined effect of monastrol with BDNF and NT-3 also improved the crossover ratio compared with controls ( $p < 0.01$ , 50  $\mu$ g/mL;  $p < 0.001$ , 100  $\mu$ g/mL and  $p < 0.01$ , 200  $\mu$ g/mL), the increase was not significantly different from growth factors alone, or drugs alone (mean  $\pm$  SEM; unpaired student's  $t$ -test). Thus, at lower CSPG concentration, there was an indication of a potentially additive effect of monastrol with neurotrophic factors, but at higher concentrations of CSPG, this apparent combined effect was not observed.

#### **Inhibition of kinesin-5 increases axonal transport of short microtubules**

The question arises as to how the anti-kinesin-5 drugs are eliciting positive effects on axonal growth as well

as the crossing of the axon onto inhibitory molecules. Previous studies have shown that inhibition of kinesin-5 increases the frequency of short microtubule transport in the axons of juvenile sympathetic neurons (11,12). In these juvenile axons, roughly two-thirds of the short microtubule transport occurs in the anterograde direction while one-third occurs roughly in the retrograde direction. Treatment with monastrol does not change the 2:1 ratio of anterograde to retrograde movements, but roughly doubles the frequencies in both directions. The greater overall vitality of microtubule transport in the axon is presumably a factor in the capacity of the axon to grow faster when kinesin-5 is inhibited. We investigated whether these findings on microtubule transport also hold true in the case of the cultured adult neurons. Adult DRG neurons were transfected with GFP (green fluorescent protein) tubulin and allowed to grow axons in the presence of monastrol, STLC or HR22C16 for 48 h. Forty-eight hours of growth were necessary for the axons to be long enough for the microtubule transport assay to be conducted. A bleached zone was made at a distance of 50–100  $\mu$ m from the cell body and short fluorescent microtubules moving across this zone were quantified (Figure 7A). Overall, the frequency of microtubule movement events in the adult axons was less than 0.3/min (Figure 7B). The frequency of microtubule transport in adult neurons with no drug treatment is roughly 1/10 the frequency observed in the axons of juvenile neurons (11). In addition, the ratio of anterograde to retrograde movements was roughly 1:1, rather than the 2:1 ratio observed in the case of the juvenile neurons (Figure 7C). Interestingly, the frequency of anterograde microtubule transport did not increase significantly in any of the cultures treated with anti-kinesin-5 inhibitors, but the frequency of retrograde microtubule transport was significantly reduced in monastrol cultures by 45% ( $p < 0.05$ ) and in STLC cultures by 81% ( $p < 0.01$ ). Therefore, the ratio of anterograde to retrograde microtubule movements was significantly increased in neurons treated with monastrol ( $3.33 \pm 0.6$ ;  $p < 0.001$ ) and STLC ( $4.75 \pm 0.16$ ;  $p < 0.001$ ) compared to control cultures ( $0.85 \pm 0.14$ ), but remained similar in cultures treated with HR22C16 ( $1.23 \pm 0.19$ ) (mean  $\pm$  SEM; unpaired student's  $t$ -test).

To test whether neurotrophic factors impact microtubule transport, we examined the effects of BDNF and NT-3 on

**Figure 7: Inhibition of kinesin-5 enhances frequency of anterograde microtubule transport.** A) Time-lapse images of a GFP-tubulin expressing neuron reveal a short microtubule moving in the anterograde direction through a photobleached region of the axon. White arrows mark the leading and trailing ends of the microtubule. Bar, 10  $\mu$ m. B) Quantification of the frequency of microtubule transport events observed in the anterograde and retrograde directions along the axon per minute in cultures treated with monastrol, STLC and HR22C16. Monastrol and STLC decrease the frequency of retrogradely moving microtubules. Addition of BDNF/NT-3 significantly increased the frequency of anterograde microtubule transport. Addition of BDNF/NT-3 in combination with monastrol further increased the frequency of anterograde microtubule transport compared to monastrol alone or to BDNF/NT-3 alone. C) Quantification of the ratio of short microtubules transported anterogradely versus microtubules transported retrogradely through the bleached region in cultures treated with monastrol, STLC and HR22C16. Monastrol and STLC increase the ratio of anterogradely moving microtubules. Addition of BDNF/NT-3 in combination with monastrol additionally increases this ratio relative to monastrol alone. D) DRG neurons treated with DMSO, monastrol, BDNF/NT-3 alone or BDNF/NT-3 and monastrol were grown in culture for 48 h. Monastrol and the combination of monastrol and growth factors significantly increased the mean of the four longest axons. Application of BDNF/NT-3 alone did not significantly increase axonal length, \* $p < 0.05$ , \*\* $p < 0.01$ , \*\*\* $p < 0.001$ .

the frequency of microtubule movements along the axon (Figure 7B,C). We found that BDNF/NT-3 increases the frequency of anterograde microtubule movement by 75% ( $p < 0.05$ ) and decreases retrograde microtubule movement by 63% ( $p < 0.01$ ) compared to control cultures. Addition of monastrol together with BDNF/NT-3 further increases anterograde microtubule movement to 250% ( $p < 0.01$ ) and decreases retrograde microtubule movement to 38% ( $p < 0.05$ ). Moreover, the combined effect of monastrol and BDNF/NT-3 increases anterograde microtubule transport by 133% ( $p < 0.01$ ) compared to monastrol alone and by 90% ( $p < 0.01$ ) compared to BDNF/NT-3 alone. Addition of BDNF/NT-3 significantly increased the ratio of anterograde versus retrograde microtubule transport ( $4.69 \pm 0.13$ ;  $p < 0.001$ ), while addition of monastrol and BDNF/NT-3 also increased the ratio of anterograde:retrograde microtubule transport ( $5.01 \pm 0.07$ ;  $p < 0.001$ ) compared to control ( $0.85 \pm 0.14$ ). The combined effect of monastrol and BDNF/NT-3 significantly increased the ratio of anterograde:retrograde microtubule transport ( $p < 0.01$ ) compared with monastrol alone.

These results are consistent with a scenario by which axonal microtubule transport is far less robust in regenerating adult axons compared to the rapidly growing axons of juvenile neurons. Inhibiting kinesin-5 alone changes the ratio of anterograde to retrograde movements to a situation more comparable to juvenile axons, but it appears the anti-kinesin-5 drugs are only able to notably augment anterograde microtubule transport frequency when used in combination with growth factors.

Based on these results, we wondered if there might be a correlation between the robustness of microtubule transport and the rate of axonal growth. However, as shown in Figure 7D, although monastrol treatment significantly increased the length of the longest four axons by 25% ( $1458.12 \pm 94.59$  m;  $p < 0.01$ ) compared to control neurons ( $1161.96 \pm 66.5$  m) and treatment with both BDNF/NT-3 and monastrol also increased axonal length by 22% ( $1415.17 \pm 93.67$  m;  $p < 0.01$ ), there was no increase in axonal length as a result of the treatment with BDNF/NT-3 alone ( $1458.12 \pm 94.59$  m). Thus, on the basis of these results, we cannot conclude that axonal growth rate is directly correlated with the robustness of microtubule transport.

#### ***Inhibition of kinesin-5 enhances microtubule entry into the distal regions of adult axons***

Developing axons are tipped by broad actin-based lamellar structures called growth cones. Inhibition of kinesin-5 prevents the microtubule array in the growth cone from being polarized which impairs the ability of the growth cone to turn in response to environmental cues (12). To investigate whether a similar situation may be at play in adult neurons challenged with an inhibitory border, we first examined adult axonal tips turning or growing in close proximity to CSPG borders under higher magnification (Figure 8A). Adult DRG axons often form dystrophic

end bulbs when growing on or near CSPG surfaces, with very little actin and no distinct peripheral or central domain (23). The dystrophic end bulbs are highly dynamic and mimic the morphology of regenerating axons growing toward the glial scar *in vivo*. We found this to be true in our cultures of adult DRG neurons, as there was a great deal of variation in dystrophic bulb size, number of filopodia and number of lamellipodial membrane ruffles. However, addition of monastrol did not significantly change any of these morphological characteristics. Moreover, on cultures immunostained to reveal microtubules, we did not observe any notable differences in microtubule organization or distribution in response to the anti-kinesin-5 drugs.

Given that still images of fixed samples are often not sufficient to reveal changes in microtubule behaviors, we also used the EB3 (end binding protein 3) comet approach (see *Materials and Methods*), in similar fashion to our earlier studies on juvenile sympathetic neurons. In these previous studies, we observed a dramatic increase in the number of EB3 comets invading the distal regions of the growth cone when monastrol was added to the cultures (12). Although some distal tips of adult DRG axons are enlarged and have lamellipodia, most are modest in size and blunt in shape and display very few filopodia. The comets that enter the tips of these axons stop at the blunt ends and very few move into the filopodia (Figure 8B). The number of comets entering the most distal region of the axonal tip was significantly increased in neurons (Figure 8C) treated with monastrol ( $19 \pm 2.65$ /min;  $p < 0.05$ ), STLC ( $19 \pm 2.66$ /min;  $p < 0.05$ ) and HR22C16 ( $18 \pm 2.74$ /min;  $p < 0.05$ ), compared to control growth cones ( $12 \pm 0.95$ ) ( $n = 10$ ; mean  $\pm$  SEM; unpaired student's *t*-test). The percentage of EB3 comets moving anterogradely in the distal 30 m portion of the axon also increased (Figure 8D) in cultures treated with monastrol ( $83 \pm 4.1\%$ ;  $p < 0.01$ ), STLC ( $78 \pm 3.88\%$ ;  $p < 0.05$ ) and HR22C16 ( $75 \pm 1.52\%$ ;  $p < 0.05$ ) (mean  $\pm$  SEM; unpaired student's *t*-test). However, the velocity of EB3 comets did not change after addition of drugs and nor did the number of comets enter filopodia (data not shown).

In contrast to the data on microtubule transport, we did not find that combined effects of monastrol with BDNF/NT-3 caused any significant increase of EB3 comet movement or changes in directionality compared with addition of monastrol alone. Surprisingly, addition of BDNF/NT-3 with monastrol actually decreased the number of comets entering the filopodia compared to monastrol alone or growth factors alone. The combination of monastrol with BDNF/NT-3 increased the percentage of anterogradely moving comets at the distal end of axons ( $87 \pm 4.4\%$ ;  $p < 0.01$ ) compared with controls ( $69 \pm 1.76\%$ ), but again, failed to cause a significantly greater increase compared to monastrol or growth factors alone. This is consistent with lack of evidence for the combination of monastrol with the growth factors displaying combinatorial positive impact on axonal crossing at most CSPG concentrations.

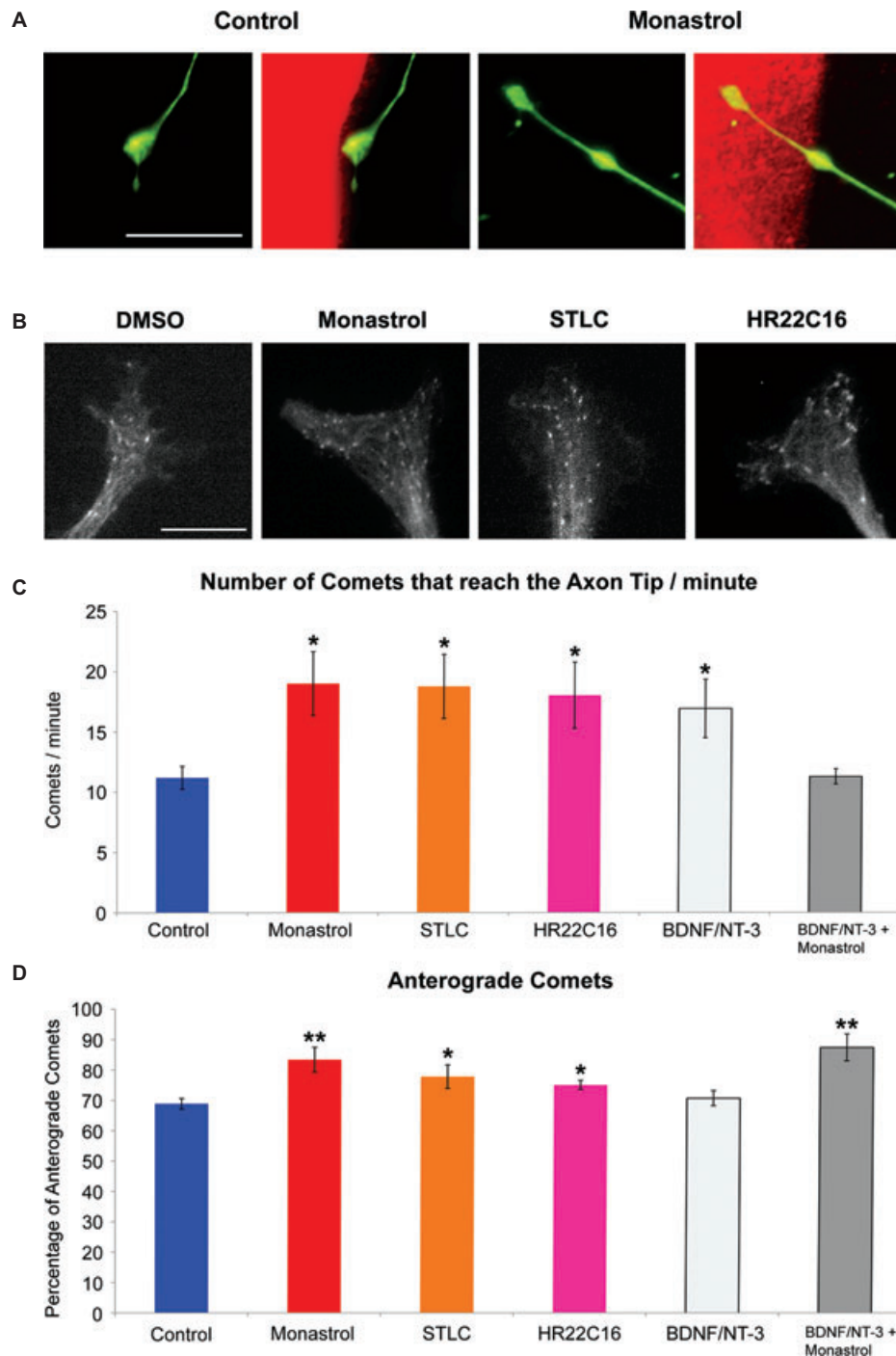


**Figure 8: Microtubule entry into the distal tip of the axon is enhanced after treatment with kinesin-5 inhibitors.** A) Axon tips which grow close to or onto the CSPG border form swellings known as dystrophic end bulbs. Immunolabeling with  $\beta$ -III tubulin (green) does not reveal any difference in microtubule distribution or morphological change in neurons treated with monastrol. Bar, 10  $\mu$ m. B) Fluorescence micrographs representative of adult DRG neurons, grown on laminin in the absence of CSPG, transfected with GFP-EB3 and treated with DMSO, monastrol, STLC or HR22C16. Bar, 10  $\mu$ m. C) Graph shows the number of EB3 comets that arrive at the distal tip of the axon per minute in neurons treated with each drug. Drug-treated neurons have a significantly higher number of EB3 comets reaching the tip of the axon compared to control neurons. BDNF/NT-3 in combination with monastrol results in a decrease in the number of comets that arrive at the distal tip of axons. D) Graph shows the percentage of anterogradely moving EB3 comets in the distal 30  $\mu$ m of the axon. Drug-treated neurons have a significantly higher proportion of anterograde EB3 comets compared to control neurons. BDNF/NT-3 in combination with monastrol does not significantly increase the proportion of anterogradely moving EB3 comets in the distal portion of the adult DRG axon compared with monastrol alone, \* $p < 0.05$ , \*\* $p < 0.01$ , \*\*\* $p < 0.001$ .

## Discussion

Drugs that target kinesin-5 are being developed as anti-cancer agents (13,14). The idea that such drugs should have no effects on the adult nervous system appears to have come from studies on mRNA levels, such as our own earlier findings using *in situ* hybridization, showing almost undetectable levels of kinesin-5 mRNA in adult rodent brain (15). However, mRNA levels do not always accurately reflect protein levels, particularly in the case of neurons, where proteins often degrade slowly so that they can persist within ribosome-deficient axoplasm (29,30). We have shown here that kinesin-5 protein is present in adult neurons, *albeit* at markedly lower levels compared to development. The fact that kinesin-5 is higher in adult neurons of the CNS than the PNS may be a factor in why CNS neurons are intrinsically poorer at regeneration than PNS neurons (1,2). Indeed, adult PNS axons grow better than CNS axons after transection, even when presented with the same permissive environments *in vitro* (31). While we are not able to study CNS neurons in culture for practical reasons, the persistent expression of kinesin-5 in the adult CNS inspires hope that whatever positive effects we see on PNS neurons could be even more robust on CNS neurons.

The two main challenges for regeneration are to induce the injured axons to grow faster and to overcome inhibitory molecules. In theory, kinesin-5 inhibition elicits effects that should be favorable toward meeting both of these goals. We found that anti-kinesin-5 drugs caused the axons of cultured adult DRG neurons to grow faster. When the axons were challenged to cross onto inhibitory CSPGs, the drugs enhanced the crossing. These results indicate that inhibiting kinesin-5 provides advantages to adult neurons both in terms of axonal growth and overcoming inhibitory obstacles.

We next wondered if inhibiting kinesin-5 might provide an additional boost when used in combination with already documented approaches for augmenting regeneration. With regard to the capacity of the axon to overcome inhibitory obstacles, one effective strategy has been to enzymatically digest the CSPGs, which then permits an increase in axonal crossing (32). We found that adding anti-kinesin-5 drugs boosted this effect when the CSPG digestion was only partial. We also observed a boost when anti-kinesin-5 drugs were combined with neurotrophins, but this was only observed at the lowest CSPG concentration in our experiments.

Perhaps of most interest to cell biologists is the underlying mechanism by which inhibiting kinesin-5 elicits its positive effects. Adult neurons grow more slowly than juvenile neurons and display far less robust microtubule transport than juvenile neurons. In addition, the ratio of anterograde:retrograde transport of microtubules is roughly 1:1 in the adult axons compared to 2:1 in the juvenile axons. We suspect that the slower growth and less robust

microtubule transport are due in part to lower expression of proteins that influence microtubule transport, such as cytoplasmic dynein (33), which we believe is the principal motor for transporting microtubules anterogradely within the axon (9). Interestingly, partial experimental depletion of cytoplasmic dynein from juvenile neurons results in a ratio of anterograde to retrograde transport that is roughly 1:1 (34) the same ratio as observed in the adult axons studied here. Two of the three anti-kinesin-5 drugs result in a strong change in the anterograde:retrograde ratio to favor anterograde transport even more so than the case with juvenile neurons, although the total frequency of microtubule transport events is still far less than in juvenile axons. The third drug's effects were similar but less robust. The growth factors produced a similar effect to these drugs on the ratio but with a far stronger increase in total microtubule transport frequency. There was an even greater effect on microtubule transport when kinesin-5 was inhibited together with the growth factors.

To date, it has never been entirely clear to what extent the rate of axonal growth correlates with the robustness of microtubule transport within the axon. The fact that the frequency of microtubule transport in the axons of these slower-growing cultured adult neurons is 1/10th the frequency of juvenile neurons in culture suggests that such a correlation may exist. However, in our previous studies, we documented similar microtubule transport frequencies in the axons of cultured rat sympathetic and hippocampal neurons, despite the fact that the former grow much faster than the latter (11,35). Moreover, the addition of BDNF/NT-3 to the adult neurons produces a dramatic increase in microtubule transport frequency with no detectable augmentation in axonal growth rate. While this issue will require more study before conclusions can be drawn with clarity, these observations suggest that the changes in microtubule transport produced by the anti-kinesin-5 drugs may not be the critical factor in explaining the more rapid growth rates of the axon. One possibility is that the impact of the drugs on the longer stationary microtubules is more relevant to axonal growth rates in that these microtubules are the ones critical for preventing the axon from retracting (11,36). Fewer bouts of retraction, even relatively short ones that occur as axons grow, would cumulatively result in longer axons. Another possibility is that the robustness of microtubule transport is a key determinant of axonal growth rate but that an increase in microtubule transport has to be coupled to other effects, for example, on the long microtubules, in order for the axon to grow faster.

The impact of the drugs on overcoming inhibitory molecules probably has less to do with the transport of short microtubules and more to do with the capacity of microtubules to invade the distal tip of the axon, which we have posited is regulated by the balance of motor-driven forces on the longer microtubules (9). The turning of the growth cone during development depends on microtubules entering the side of the growth cone toward the

direction of the turn (37). Kinesin-5 is thought to be critical for this to occur because it suppresses microtubules from entering the other side of the growth cone (12). However, adult axonal tips are much smaller in size and are much less motile than juvenile growth cones. Treatments that augment entry of microtubules throughout the tip of the axon presumably prevent the cytoskeletal apparatus from steering the axon away from the inhibitory substrate. Our studies indicate that either treatment with the growth factors or the anti-kinesin-5 drugs enhance microtubule entry into the distal tip of the axon. As with the microtubule transport results, we suspect that the impact of inhibiting kinesin-5 is less impressive than with juvenile neurons because there is less kinesin-5 to inhibit in the case of the adult. Surprisingly, not only was there no additive effect of combining the growth factors with the anti-kinesin-5 drugs, but there also appeared to be less total entry of microtubules into the distal axon than with either treatment alone.

In terms of clinical use for treating nerve injury, anti-kinesin-5 drugs might have other advantageous effects, such as limiting proliferation of lymphocytes, macrophages and microglia, which are released from the glial scar and cause pain and inflammatory tissue damage in the secondary phase of nerve injury (38,39). However, there are caveats worth noting as well. For example, the drug treatment may well enable axons to overcome inhibitory molecules, but the axon may also be unresponsive to positive environmental cues that route the axon to its target. Excessive branching or sprouting could also be a problem, for example, with axons that transmit pain sensations. At present, there are no overt indications that the anti-kinesin-5 drugs produce any toxic or non-specific effects on neurons, even at rather high concentrations. However, the possibility for such effects still remains. For example, the variability in drug effects observed with the different anti-kinesin-5 drugs (e.g. HR22C16 not impacting retrograde microtubule transport nearly as much as the other drugs) may relate to differences in non-specificity or toxicity among the drugs. Such effects could potentially be a greater factor with more prolonged treatments. These and other issues will have to be tested in an *in vivo* experimental regime for nerve injury.

In conclusion, the present work suggests that anti-kinesin-5 drugs may be useful for augmenting nerve regeneration after injury. The effects of the drugs are clearly less impressive on adult neurons than with juvenile neurons, presumably because there is less kinesin-5 to inhibit. The next step for testing the efficacy of the drugs would be to utilize them in an *in vivo* model of nerve injury, as nerve regeneration is a complicated business involving a number of intersecting factors. In addition, the insights provided by the present studies may be useful in devising other approaches for enhancing the capacity of the microtubule array to participate in faster axonal growth and greater invasiveness of the axonal tip into inhibitory environments.

## Materials and Methods

### Animals

Mice (C57BL/6J; 20–25 g; Jackson Laboratories) were used for all experiments except for quantitative RT-PCR. Quantitative studies on baseline kinesin-5 levels in various tissues were performed at ages ranging from embryonic to adult, taken from non-injured animals. For studies on conditional dorsal root injury, young adult mice (C57BL/6J; 20–25 g; Jackson Laboratories) were used, with at least three animals in each experimental group. For cell culture work, non-injured adult mice were used. The RT-PCR experiments were conducted using male and female Sprague Dawley rats (new born and adults, 180–200 g).

### Semi-quantitative and RT-PCR

Three rats were sacrificed at 3, 7, 14 and 90 days postnatal. The cerebral cortex was collected from the rats and used for total RNA extraction using Trizol reagent (Invitrogen). Total RNA (1  $\mu$ g) was used in a reverse transcription reaction (Omniscript RT Kit; Qiagen, Inc.). Primers were designed against the whole sequences for rat kinesin-5 and GAPDH, respectively. GAPDH-sense: 5'-gcctccgtgttctacc-3' and antisense: 5'-gctgcttcaccaccttc-3'; kinesin-5-sense: 5'-acactgtgagaactgaacc-3' and antisense: 5'-cagggctcttgacttacg-3' were synthesized by Invitrogen. Semi-quantitative PCR was done in a 25  $\mu$ L mixture using a PCR kit (Fermentas) and performed in a thermal cycler (Eppendorf). RT-qPCR was performed and analyzed with a StepOne RT-PCR system (Applied Biosystems). The mRNA quantity of kinesin-5 or GAPDH was automatically calculated based on the fluorescence data acquired after each thermocycle.

### Conditional dorsal root crush

Adult female mice were anesthetized by intraperitoneal injection of ketamine (120 mg/kg; Fort Dodge Laboratories) and xylazine (4 mg/kg; Lloyd Laboratories). Under aseptic conditions a mid-thigh incision fully exposed the sciatic nerve, proximal to the tibial/peroneal division. Both the left and right sciatic nerves were crushed using fine forceps for 10 seconds. The muscle was then closed using sutures and the skin was secured with two staples. After 10 days, animals were anesthetized and L5 dorsal roots were exposed. Using a surgical microscope, the dura was pierced and the dorsal roots were crushed using fine forceps for 10 seconds on the left and right side. A subdural bio-membrane (Bertek Pharmaceuticals, Inc.) was placed over the exposed region of spinal cord before the muscles were closed using sutures and the skin was secured using staples. Mice were rehydrated after surgery with 0.5 mL saline solution (Braun Medical, Inc.) and left to recover for 2 days before being euthanized for analysis.

### Tissue collection

Mouse neural tissues from the cortex, spinal cord and DRGs were isolated at different stages of development (P1,  $n = 7$ ; P7,  $n = 7$ ; P14,  $n = 6$ ; 10-week-old young adults,  $n = 3$ ) and homogenized in mammalian CellLytic™ M Cell Lysis Reagent (C3228; Sigma). A cocktail of protease inhibitors (PI-78425; Thermo Fisher Scientific) was added into the lysis reagent 1:50 dilution. In adults, injured and non-injured mouse tissues were also collected from the spinal cord, DRGs and sciatic nerves ( $n = 3$  for each condition). Tissues from the adult spinal cord and DRGs were collected from the L4-6 spinal cord segments and L4-6 DRGs (proximal to the L5 dorsal root injury site) or from other segments of the spinal cord and other DRGs from the lumbar to sacral levels (distal to the L5 dorsal root injury site). The proteins were quantified before being homogenized in Laemli's sample buffer using 1  $\mu$ L of buffer/1  $\mu$ g of protein.

### Kinesin-5 antibodies

For western blotting, a novel polyclonal anti-kinesin-5 antibody (DCM-22) was raised in rabbits (Cocalico Biologicals, Inc.) against the tail domain of rat kinesin-5 (amino acid residues 801-991, protein derived from Genbank XP\_001060913.1). The anti-serum was affinity purified on IgG covalently

bound to a HiTrap column (GE Healthcare Life Sciences) following the GE company's protocol. For immunostaining, a rabbit anti-kinesin-5 antibody was purchased from Abcam (ab61199), raised against an epitope containing Thr 927 in mouse kinesin-5. Both antibodies worked for blotting and immunostaining, but the properties of our DCM-22 antibody were better for blotting while the properties of the Abcam antibody were better for immunostaining.

### Western blotting of mouse tissues

Proteins (5 g cortex, 20 g spinal cord, 15 g DRG and 15 g sciatic nerve) were separated by SDS-PAGE using 7.5% gels. To confirm the identity of the band produced by the kinesin-5 antibody from these tissues, an RFL-6 was cultured for 2 days in the presence of control or kinesin-5 siRNA, according to our previous methods (11). The cell lysates (10 g) were run alongside mouse tissue samples and probed with the same anti-kinesin-5 antibody to show that the band corresponding to kinesin-5 was diminished by the siRNA. To obtain standard curves, proteins were transferred to nitrocellulose membranes after electrophoresis and blocked with 7.5% non-fat milk solids before immunoblotting with anti-kinesin-5 DCM-22 antibody (1:500) and anti-GAPDH antibody, for loading controls (1:2500; G8795; Sigma). Optical density (OD) readings were measured for each protein band corresponding to a different stage in development and repeated for three different tissue samples using the GENESNAP and GENETOOLS software (SynGene Group). Films were imaged using a Syngene Chromascan scanner (SynGene Group). The OD readings of the bands corresponding to kinesin-5 were standardized according to the GAPDH loading control and according to the exposure length of the film.

### Immunohistochemistry on mouse tissues

Non-injured and injured mice were perfused transcardially with 4% paraformaldehyde prior to dissecting the spinal cord (2 mm rostral and 2 mm caudal to the L5 dorsal root), DRGs (L4, L5, L6 and S1) and sciatic nerves. After postfixation in the same fixative for 1 h, tissues were transferred to a 30% sucrose solution and left overnight before embedding in M1 mounting medium (Thermo Fisher Scientific). Tissues were cut frozen at  $-20^{\circ}\text{C}$  on a cryostat (Leica). The spinal cord was cut coronally (20  $\mu\text{m}$  thick) from 1 mm caudal to 1 mm rostral of the L4/L5 DREZ (dorsal root entry zone). The sciatic nerve was cut longitudinally into 20  $\mu\text{m}$  thick sections and DRGs were cut into 15  $\mu\text{m}$  thick sections. Tissue sections were prepared according to a previous publication (40) and stained with anti-kinesin-5 antibody (1:400; Abcam), NeuN (1:100; Millipore), S-100 monoclonal antibody (1:100; Millipore) or SMI-31R (1:1000; Covance). Some sections were also incubated with the NeuroTrace™ fluorescent Nissl stain (1:300; Molecular Probes). To control for non-specific antibody binding, sections were incubated with blocking buffer overnight, followed by only the secondary antibody (data not shown).

### Cell culture CSPG stripe assay

Circular glass coverslips with predrilled 14 mm wells (MatTek Corporation) were coated with poly-D-lysine overnight. A strip of Whatman filter paper (10  $\times$  1 mm) was fully saturated with 6  $\mu\text{L}$  of aggrecan solution (25, 50, 100 or 200  $\mu\text{g}/\text{mL}$ ; Sigma) placed at the center of the coverslip for 30 min and allowed to air-dry as a modification of a previous technique (41). The coverslips were coated with laminin (60  $\mu\text{g}/\text{mL}$ ) and kept at  $37^{\circ}\text{C}$  for 3 h. Some coverslips were incubated in ChABC diluted in water (0.1 U/mL; Sekagaku) at  $37^{\circ}\text{C}$  for 3 h. These conditions were all chosen empirically after testing the effects of various incubation times and concentrations of aggrecan, laminin and ChABC. Our goal was to allow enough time for some digestion of CSPG GAG chains, but not enough time for all the GAG chains to be inactivated. This could be tested with the CS-56 antibody, which recognizes the remaining intact CSPG GAGs. The coverslips were washed in culture medium, dried and UV sterilized before DRG cells were plated.

### Cell culture and pharmacology

DRGs from adult C57B1/6j mice (Jackson Laboratories) were isolated and cultured as described previously (42) onto stripe assay coverslips (4000

cells/coverslip). All growth factors and pharmacological reagents were added directly to the culture medium at indicated concentration shortly after the cells adhered to the substratum. For growth factor treatment, cells were incubated in DRG medium containing 300 ng/mL BDNF and 20 ng/mL NT-3 (Peprotech). For anti-kinesin-5 drugs, monastrol (100  $\mu\text{M}$ ), STLC (10  $\mu\text{M}$ ) and HR22C16 (10  $\mu\text{M}$ ; EMD4Biosciences) were added to the media 3 h after plating. Coverslips were replenished with the same culture media after 24 h and fixed at 48 h. For cell morphology observations some cultures were fixed at 18 h.

### Immunocytochemistry on cell neuronal cultures

Immunostaining of cell cultures was done as previously described (36). To control for non-specific antibody binding and auto-fluorescence of neurons, cultures were incubated with only the secondary antibodies or with no antibodies. Immunofluorescence was negligible in these dishes (data not shown).

### Image analysis

For consistency, images were taken from regions in which cell density, axonal outgrowth and number of cell bodies around the CSPG border were similar between control- and drug-treated cultures. Images were obtained on an Axiovert 200 microscope (Carl Zeiss) equipped with a high-resolution charge-coupled device (CCD; Orca ER). All images were obtained using identical camera, microscope and imaging criteria such as gain, exposure time, brightness and contrast. Digital gray values of image pixels representing arbitrary fluorescence units were obtained using AXIOVISION software. In cases where multiple axons grew from a single DRG cell body, the four longest axons were measured and the sum of the length of all four axons was calculated. A mean of the total length of four axons was calculated for all the cells in each condition.

### Characterization of DRG axonal crossing behavior

Representative digital images of CSPG borders where CSPG (identified with CS-56 antibody) and neurons (identified using anti- $\beta$ -III tubulin antibody) were collected with a 25 $\times$  objective. Each image was standardized to include roughly equal proportions of an area inside and outside the CSPG border. Growth in and around the border was quantified using equal sized rectangular boxes (4000 pixels<sup>2</sup>) placed side by side along the border and at small distances away from the border. The mean pixel intensity in the rectangles, labeled by tubulin on the laminin side and on the CSPG side was recorded using the ZEISS AXIOVISION REL. 4.6 software. To eliminate background, the mean pixel area in the darkest corner of each image, not representing neuronal growth, was quantified with a smaller box (200 pixels<sup>2</sup>). Average threshold pixel densities were calculated per each treatment group and compared using a student's *t*-test, assuming unequal variances.

### Microtubule transport assay

The microtubule transport assay was performed essentially as described previously (11), except adult DRG neurons were plated onto laminin coverslips and imaged 48 h later. Images were taken at 300 milliseconds exposure using 3-second intervals for each axon. Transport analysis included all microtubules observed to move continuously through the photobleached region during the imaging period. Transport frequencies were calculated by dividing the total number of movements by the total imaging time for individual movies.

### GFP-EB3 imaging

EB3 is a microtubule end-binding protein that associates with the plus end of the microtubule during bouts of assembly, and hence, GFP-EB3 appears as fluorescent 'comets' at the plus ends of the assembling microtubules (43). Ectopic expression of GFP-EB3 has proven to be a convenient approach for visualizing microtubule assembly events in living neurons. Dissociated adult mouse dorsal root ganglia were transfected using the Amaxa Nucleofector (Amaxa Biosystems) with 0.3 ng of GFP-EB3 (provided by Dr Niels Galjart, Erasmus Medical Center) to visualize

EB3 comets. DMSO, monastrol, STLC or HR22C16 were added to the medium after the cells had settled down. Images were acquired 18 h later. Images of the distal portion of axons were obtained every second for 3 min at an exposure time of 150 milliseconds, as described previously (12,16). The images were quantified for the number of comets that reached the growth cone peripheral domain every minute.

### Statistical analysis

Data were analyzed using MICROSOFT EXCEL 2004 data analysis toolkit (version 11.0 for MAC, Microsoft, Inc.). Analyses of variation using paired or unpaired two-sample *t*-tests were used where appropriate.  $p < 0.05$  was considered statistically significant and data are represented as the mean  $\pm$  SEM.

### Acknowledgments

This work was funded by a grant from the Christopher and Dana Reeve Foundation to P. W. B., a grant from the Craig H. Neilsen Foundation to W. Y., a collaborative grant from the Christopher and Dana Reeve Foundation to P. W. B. and D. M. S. and a grant from the NIH to P. W. B. S. L. was funded by a postdoctoral fellowship from the Craig H. Neilsen Foundation. We are grateful to Vidya Nadar, Ronghua Wu, Gianluca Gallo, Christopher Calulut and Marion Murray for helpful input.

### References

- Abe N, Cavalli V. Nerve injury signaling. *Curr Opin Neurobiol* 2008;18:276–283.
- Huebner EA, Strittmatter SM. Axon regeneration in the peripheral and central nervous systems. *Results Probl Cell Differ* 2009;48:339–351.
- Silver J, Miller JH. Regeneration beyond the glial scar. *Nat Rev Neurosci* 2004;5:146–156.
- Giger RJ, Venkatesh K, Chivatakarn O, Raiker SJ, Robak L, Hofer T, Lee H, Rader C. Mechanisms of CNS myelin inhibition: evidence for distinct and neuronal cell type specific receptor systems. *Restor Neurol Neurosci* 2008;26:97–115.
- Lu P, Tuszynski MH. Growth factors and combinatorial therapies for CNS regeneration. *Exp Neurol* 2008;209:313–320.
- Verma P, Chierzi S, Codd AM, Campbell DS, Meyer RL, Holt CE, Fawcett JW. Axonal protein synthesis and degradation are necessary for efficient growth cone regeneration. *J Neurosci* 2005;25:331–342.
- Hoffman PN. A conditioning lesion induces changes in gene expression and axonal transport that enhance regeneration by increasing the intrinsic growth state of axons. *Exp Neurol* 2010;223:11–18.
- Wang L, Brown A. Rapid movement of microtubules in axons. *Curr Biol* 2002;12:1496–1501.
- Baas PW, Vidya Nadar C, Myers KA. Axonal transport of microtubules: the long and short of it. *Traffic* 2006;7:490–498.
- Peterman EJ, Scholey JM. Mitotic microtubule crosslinkers: insights from mechanistic studies. *Curr Biol* 2009;19:R1089–R1094.
- Myers KA, Baas PW. Kinesin-5 regulates the growth of the axon by acting as a brake on its microtubule array. *J Cell Biol* 2007;178:1081–1091.
- Nadar VC, Ketschek A, Myers KA, Gallo G, Baas PW. Kinesin-5 is essential for growth-cone turning. *Curr Biol* 2008;18:1972–1977.
- Luo L, Parrish CA, Nevins N, McNulty DE, Chaudhari AM, Carson JD, Sudakin V, Shaw AN, Lehr R, Zhao H, Sweitzer S, Lad L, Wood KW, Sakowicz R, Annan RS et al. ATP-competitive inhibitors of the mitotic kinesin KSP that function via an allosteric mechanism. *Nat Chem Biol* 2007;3:722–726.
- Huszar D, Theoclitou ME, Skolnik J, Herbst R. Kinesin motor proteins as targets for cancer therapy. *Cancer Metastasis Rev* 2009;28:197–208.
- Ferhat L, Cook C, Chauviere M, Harper M, Kress M, Lyons GE, Baas PW. Expression of the mitotic motor protein Eg5 in postmitotic neurons: implications for neuronal development. *J Neurosci* 1998;18:7822–7835.
- Vogelaar CF, Hoekman MF, Gispen WH, Burbach JP. Homeobox gene expression in adult dorsal root ganglia during sciatic nerve regeneration: is regeneration a recapitulation of development? *Eur J Pharmacol* 2003;480:233–250.
- Takemura R, Nakata T, Okada Y, Yamazaki H, Zhang Z, Hirokawa N. mRNA expression of KIF1A, KIF1B, KIF2, KIF3A, KIF3B, KIF4, KIF5, and cytoplasmic dynein during axonal regeneration. *J Neurosci* 1996;16:31–35.
- Mayer TU, Kapoor TM, Haggarty SJ, King RW, Schreiber SL, Mitchison TJ. Small molecule inhibitor of mitotic spindle bipolarity identified in a phenotype-based screen. *Science* 1999;286:971–974.
- DeBonis S, Skoufias DA, Lebeau L, Lopez R, Robin G, Margolis RL, Wade RH, Kozielski F. *In vitro* screening for inhibitors of the human mitotic kinesin Eg5 with antimetastatic and antitumor activities. *Mol Cancer Ther* 2004;3:1079–1090.
- Hotha S, Yarrow JC, Yang JG, Garrett S, Renduchintala KV, Mayer TU, Kapoor TM. HR22C16: a potent small-molecule probe for the dynamics of cell division. *Angew Chem Int Ed Engl* 2003;42:2379–2382.
- Steinmetz MP, Horn KP, Tom VJ, Miller JH, Busch SA, Nair D, Silver DJ, Silver J. Chronic enhancement of the intrinsic growth capacity of sensory neurons combined with the degradation of inhibitory proteoglycans allows functional regeneration of sensory axons through the dorsal root entry zone in the mammalian spinal cord. *J Neurosci* 2005;25:8066–8076.
- Snow DM, Lemmon V, Carrino DA, Caplan AI, Silver J. Sulfated proteoglycans in astroglial barriers inhibit neurite outgrowth *in vitro*. *Exp Neurol* 1990;109:111–130.
- Tom VJ, Steinmetz MP, Miller JH, Doller CM, Silver J. Studies on the development and behavior of the dystrophic growth cone, the hallmark of regeneration failure, in an *in vitro* model of the glial scar and after spinal cord injury. *J Neurosci* 2004;24:6531–6539.
- Moon LD, Asher RA, Rhodes KE, Fawcett JW. Regeneration of CNS axons back to their target following treatment of adult rat brain with chondroitinase ABC. *Nat Neurosci* 2001;4:465–466.
- Kwok JC, Afshari F, Garcia-alias G, Fawcett JW. Proteoglycans in the central nervous system: plasticity, regeneration and their stimulation with chondroitinase ABC. *Restor Neurol Neurosci* 2008;26:131–145.
- Jones LL, Margolis RU, Tuszynski MH. The chondroitin sulfate proteoglycans neurocan, brevican, phosphacan, and versican are differentially regulated following spinal cord injury. *Exp Neurol* 2003;182:399–411.
- Lee H, McKeon RJ, Bellamkonda RV. Sustained delivery of thermostabilized chABC enhances axonal sprouting and functional recovery after spinal cord injury. *Proc Natl Acad Sci U S A* 2010;107:3340–3345.
- Edstrom A, Ekstrom PA, Tonge D. Axonal outgrowth and neuronal apoptosis in cultured adult mouse dorsal root ganglion preparations: effects of neurotrophins, of inhibition of neurotrophin actions and of prior axotomy. *Neuroscience* 1996;75:1165–1174.
- Couchie D, Legay F, Guilleminot J, Lebarry F, Brion JP, Nunez J. Expression of Tau protein and Tau mRNA in the cerebellum during axonal outgrowth. *Exp Brain Res* 1990;82:589–596.
- Aronov S, Aranda G, Behar L, Ginzburg I. Axonal tau mRNA localization coincides with tau protein in living neuronal cells and depends on axonal targeting signal. *J Neurosci* 2001;21:6577–6587.
- Chierzi S, Ratto GM, Verma P, Fawcett JW. The ability of axons to regenerate their growth cones depends on axonal type and age, and is regulated by calcium, cAMP and ERK. *Eur J Neurosci* 2005;21:2051–2062.
- Del Rio JA, Soriano E. Overcoming chondroitin sulphate proteoglycan inhibition of axon growth in the injured brain: lessons from chondroitinase ABC. *Curr Pharm Des* 2007;13:2485–2492.
- Pfister KK, Shah PR, Hummerich H, Russ A, Cotton J, Annuar AA, King SM, Fisher EM. Genetic analysis of the cytoplasmic dynein subunit families. *PLoS Genet* 2006;2:e1.
- He Y, Francis F, Myers KA, Yu W, Black MM, Baas PW. Role of cytoplasmic dynein in the axonal transport of microtubules and neurofilaments. *J Cell Biol* 2005;168:697–703.
- Qiang L, Yu W, Liu M, Solowska JM, Baas PW. Basic fibroblast growth factor elicits formation of interstitial axonal branches via enhanced severing of microtubules. *Mol Biol Cell* 2010;21:334–344.

36. Myers KA, Tint I, Nadar CV, He Y, Black MM, Baas PW. Antagonistic forces generated by cytoplasmic dynein and myosin-II during growth cone turning and axonal retraction. *Traffic* 2006;7:1333–1351.
37. Geraldo S, Gordon-Weeks PR. Cytoskeletal dynamics in growth-cone steering. *J Cell Sci* 2009;122:3595–3604.
38. Watkins LR, Milligan ED, Maier SF. Glial activation: a driving force for pathological pain. *Trends Neurosci* 2001;24:450–455.
39. Milligan ED, Twining C, Chacur M, Biedenkapp J, O'Connor K, Poole S, Tracey K, Martin D, Maier SF, Watkins LR. Spinal glia and proinflammatory cytokines mediate mirror-image neuropathic pain in rats. *J Neurosci* 2003;23:1026–1040.
40. Son YJ, Thompson WJ. Schwann cell processes guide regeneration of peripheral axons. *Neuron* 1995;14:125–132.
41. Lagenaur C, Lemmon V. An L1-like molecule, the 8D9 antigen, is a potent substrate for neurite extension. *Proc Natl Acad Sci U S A* 1987;84:7753–7757.
42. Malin SA, Davis BM, Molliver DC. Production of dissociated sensory neuron cultures and considerations for their use in studying neuronal function and plasticity. *Nat Protoc* 2007;2:152–160.
43. Stepanova T, Slemmer J, Hoogenraad CC, Lansbergen G, Dortland B, De Zeeuw CI, Grosveld F, van Cappellen G, Akhmanova A, Galjart N. Visualization of microtubule growth in cultured neurons via the use of EB3-GFP (end-binding protein 3-green fluorescent protein). *J Neurosci* 2003;23:2655–2664.